Research Article

Guiqing Zhao, Ruoyan Li, Xiangdong Xing, Jiantao Ju*, Xinyi Li, and Jian Zu

Removal behavior of Zn and alkalis from blast furnace dust in pre-reduction sinter process

https://doi.org/10.1515/gps-2023-0045
received March 10, 2023; accepted June 12, 2023

Abstract: In this study, iron concentrate and blast furnace dust were used as raw materials, and graphite was used as a reducing agent for mixing and briquetting. The briquettes were roasted in a high-temperature tube furnace at different temperatures and held for a certain time to simulate the pre-reduction sintering process. The effects of dust content, reduction time, and reduction temperature on the removal rate of zinc, potassium, and sodium and the metallization rate of the pre-reduction sintered products were investigated. The reduced briquettes were characterized by X-ray diffraction, scanning electron microscopy-energy dispersive spectroscopy, and flame atomic absorption spectroscopy to further explore the mechanisms of zinc, potassium, and sodium removal. The Zn removal rate and metallization rate increased gradually with the increase in dust content, reaching 97.57% and 87.14% at 30% dust content, respectively. Both K and Na removal rates reached a maximum of 83.57% and 94.78%, respectively, at 25% dust content. With the increase in reduction time and temperature, the removal rate of the three elements and the metallization rate gradually increased. When the briquettes with 20% blast furnace (BF) dust content were reduced at 1,200°C for 20 min, the removal rates of zinc, potassium, and sodium reached 95.66%, 79.97%, and 91.49%, respectively, and the metallization rate reached 84.77%. It shows that the pre-reduction sintering process can effectively remove Zn, K, and Na from the BF dust and meet the requirements of subsequent BF production. The research results can provide some theoretical basis for industrial production.

Keywords: pre-reduction sinter, blast furnace dust, removal rate, metallization rate, removal mechanism

*** Corresponding author: Jiantao Ju,** School of Metallurgical Engineering, Xi'an University of Architecture and Technology, Xi'an 710055, China; Research Center of Metallurgical Engineering Technology of Shaanxi Province, Xi'an 710055, China, e-mail: ju_jiantao@163.com
Guiqing Zhao: Technical Center of Jiuquan Iron and Steel (Group) Co., Ltd, Jiayuguan 735100, China
Ruoyan Li, Xiangdong Xing, Xinyi Li, Jian Zu: School of Metallurgical Engineering, Xi'an University of Architecture and Technology, Xi'an 710055, China; Research Center of Metallurgical Engineering Technology of Shaanxi Province, Xi'an 710055, China

1 Introduction

In recent years, with the rapid development of the steel industry, steel production has been increasing, but it is accompanied by the generation of a large amount of solid waste such as metallurgical dust, which is about 9–12% of crude steel production [1]. In 2021, China's crude steel output reached 1.03 billion tons, while metallurgical dust output reached 92.7–123.6 million tons. Metallurgical dust is not only rich in Fe and C elements, but also contains a large amount of Zn, K, Na, and other harmful elements [2–5]. So far, only a small amount of metallurgical dust has been effectively utilized every year [6], most of which is still accumulated in steel plants or in landfills, causing waste of resources and serious environmental pollution.

According to previous research, there are two main methods to recycle metallurgical dust, such as blast furnace (BF) dust, the pyrometallurgical process and the hydrometallurgical process. In the process of hydrometallurgy, acid leaching, alkali leaching, and ammonia leaching are usually used. However, the iron extraction efficiency of hydrometallurgical processes is low, and the removal rate of Zn and alkali metals (K and Na) is also low, usually no more than 85%. In addition, hydrometallurgical processes can produce wastewater when treating metallurgical dust [7–9]. So far, pyrometallurgical technologies such as rotary hearth furnace, rotary kiln, and direct reduction have been proven to be effective methods for recovering and treating BF dust [10–20], but with high investment and operating costs, high energy consumption, and the need for secondary treatment of metallurgical dust. In addition to the above methods, BF dust is also commonly used as a raw material for sintering. However, the conventional sintering process is less effective in dezincification and dealkalization, and Zn, K, and Na in the raw material are cyclically enriched in this process. It will not only affect the quality and output of sinter, but also damage the lining of the BF,

resulting in suspension, nodules, high energy consumption, and other consequences [21–25], which will adversely affect the normal operation of the blast furnace. Therefore, the search for a method that can directly utilize BF dust ash and simultaneously remove Zn, K, and Na has become an urgent problem [26,27].

Pre-reduction sintering is a production process in which partial reduction of iron ore occurs during the sintering process. It can transfer the partially reduced iron ore to the sintering process, which is helpful to reduce the reduction load of the BF and reduce the overall energy consumption [28]. JFE in Japan developed the pre-reduction sintering technology [29–32], which mainly added part of the iron reduction in the sintering process to save the use of BF coke and thus reduce the production of CO_2. Sato et al. [33] found that the energy consumption in the sintering process increases with the increase in reduction degree, but the energy consumption of the whole BF decreases, which is conducive to energy savings. Hu et al. [34] studied the quality index of sintered minerals and the removal rate of harmful elements by simulating the production conditions of refractory dust and normal sintered raw materials for reasonable ore allocation and pre-reduction sintering. The results show that the pre-reduction sintering method can realize the efficient separation and enrichment of harmful elements in the dust of steel mills, obtain the ideal pre-reduction sinter, and rationally use the resources. Zhu et al. [4] put forward the blast pre-reduction sintering method, and studied the migration and distribution mechanisms of Zn, Pb, and As along the vertical direction of the sinter layer and the change in zoning in the sinter layer. The results show that the pre-reduced sinter with low zinc, lead, and arsenic content can be produced by the pre-reduced sintering process. In conclusion, the pre-reduction sintering method can not only reduce energy consumption, but also remove harmful elements such as zinc from BF dust. Although past studies have confirmed the practical feasibility of this technology, the pre-reduction sintering process is still in the experimental stage. In the aspect of engineering application, some key technologies need further exploration and research.

This research is based on pre-reduction sintering theory. With BF dust and iron concentrate as raw materials and graphite powder as the reducing agent, the simulated pre-reduction sintering experiments were carried out in a high temperature tube furnace. The contents of iron, zinc, potassium, and sodium in the products were determined by chemical analysis and flame atomic absorption spectrometry (FAAS). The effects of BF dust content, reduction time, and temperature on the removal rate of zinc, potassium, and sodium and the metallization rate of pre-reduction sintered products were studied. Then, the phase composition and microstructure of the pre-reduction sintered products were characterized by X-ray diffraction (XRD) and scanning electron microscope-energy dispersive spectroscopy (SEM-EDS). The phase transition and distribution of Fe, Zn, K, and Na in the pre-reduction sintering process were analyzed, and the removal mechanism of zinc and alkali by pre-reduction sintering was expounded, which provided a theoretical basis for further industrial application. A large amount of BF dust was utilized while exploring the new process of pre-reduction sintering, which is a guide for the subsequent research.

2 Experimental method

2.1 Raw materials

The iron-containing raw materials used in this study include BF dust and three kinds of iron ore powder, which are collected from a steel mill in China. ZC and GHL are two self-produced iron concentrates from that steel plant. NM is an imported iron concentrate. Their chemical compositions are listed in Table 1. In the experiment, quicklime and limestone were used as flux, and chemical pure graphite powder was used as a reducing agent. As shown in Table 1, the three iron ore powders are iron concentrates with a high iron grade and are valuable iron-containing resources. The low grade of iron and high Zn, K, and Na content of BF dust limit its ability to be recycled through traditional steel production

Table 1: Chemical compositions of the raw materials (wt%)

Item		TFe	CaO	SiO_2	Al_2O_3	K_2O	Na_2O	ZnO	MgO	C
BF dust		28.12	5.47	9.41	3.26	4.18	0.56	7.12	1.77	22.95
Iron concentrate	ZC	52.90	2.27	8.12	1.18	0.34	0.04	0.05	3.20	—
	NM	61.28	0.17	5.27	2.69	0.02	< 0.01	0.01	0.26	—
	GHL	62.16	0.95	6.93	1.02	0.17	—	0.02	1.86	—

processes. Figure 1a–d shows the XRD patterns of four iron-containing raw materials. As shown in Figure 1, Fe in ZC is mainly in the form of magnetite (Fe_3O_4) and a small amount in the form of rhodochrosite ($FeCO_3$), and Fe in NM and GHL is mainly in the form of hematite (Fe_2O_3). The iron-bearing phase of BF dust is composed of hematite (Fe_2O_3) and a small amount of magnetite (Fe_3O_4), Zn mainly exists in the form of zinc ferrite ($ZnFe_2O_4$) and sphalerite (ZnS), while K and Na mainly exist in the form of potassium chloride (KCl) and sodium chloride (NaCl), and C is also detected. Figure 2 shows the SEM-EDS image of BF dust, which can also verify the results of the previous analysis.

2.2 Experimental methods

After drying for 2 h at 105°C to completely remove free water, all raw materials were completely mixed in accordance with the calculated ratio in Table 2 under the premise that the fixed C/O molar ratio was 1.0 to ensure the complete reduction of iron-containing oxides to iron. In the mixing process, the content of BF dust was changed (10%, 15%, 20%, 25%, and 30%) to study its influence on the removal of Zn, K, and Na in the pre-reduction sintering process, while the other mineral powder proportions were kept constant. After complete mixing, 1% of sodium carboxymethylcellulose $[C_6H_9O_5(CH_2COONa)]_n$ was added to the mixture as binder, stirred evenly, and put into the manual hydraulic molding machine for briquetting under 20 MPa pressure for 3 min. Each briquette weighs about 3 g and measures 25 mm × 25 mm × 5 mm. Due to the small amount of binder, the effect on reduction is negligible.

The prepared briquettes were placed in a corundum porcelain boat and then put into a high temperature tube furnace in a nitrogen atmosphere for a simulated pre-reduction sintering experiment. The briquettes with different BF dust contents were heated from room temperature to the set reduction temperature and held for a certain

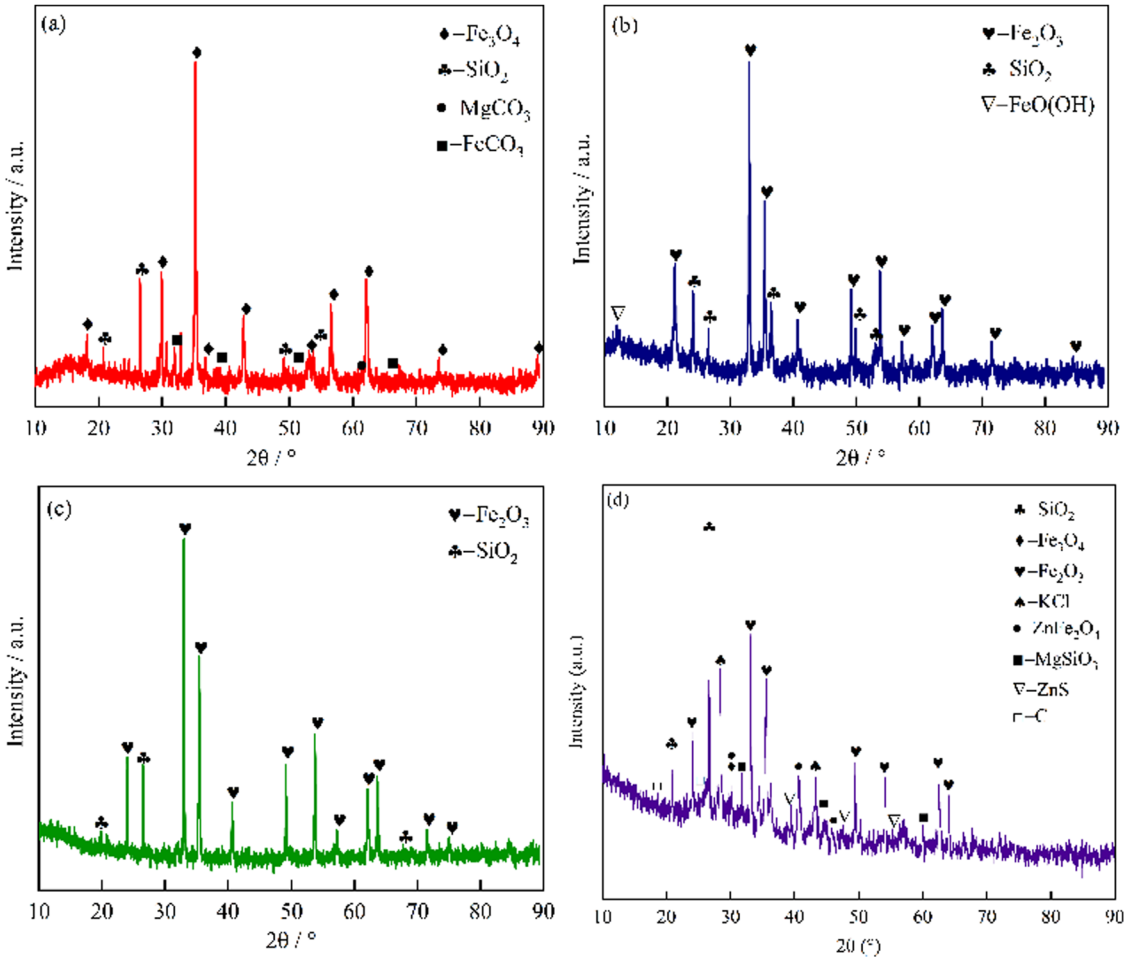

Figure 1: XRD spectrograms of the raw materials: (a–c) iron concentrate and (d) BF dust.

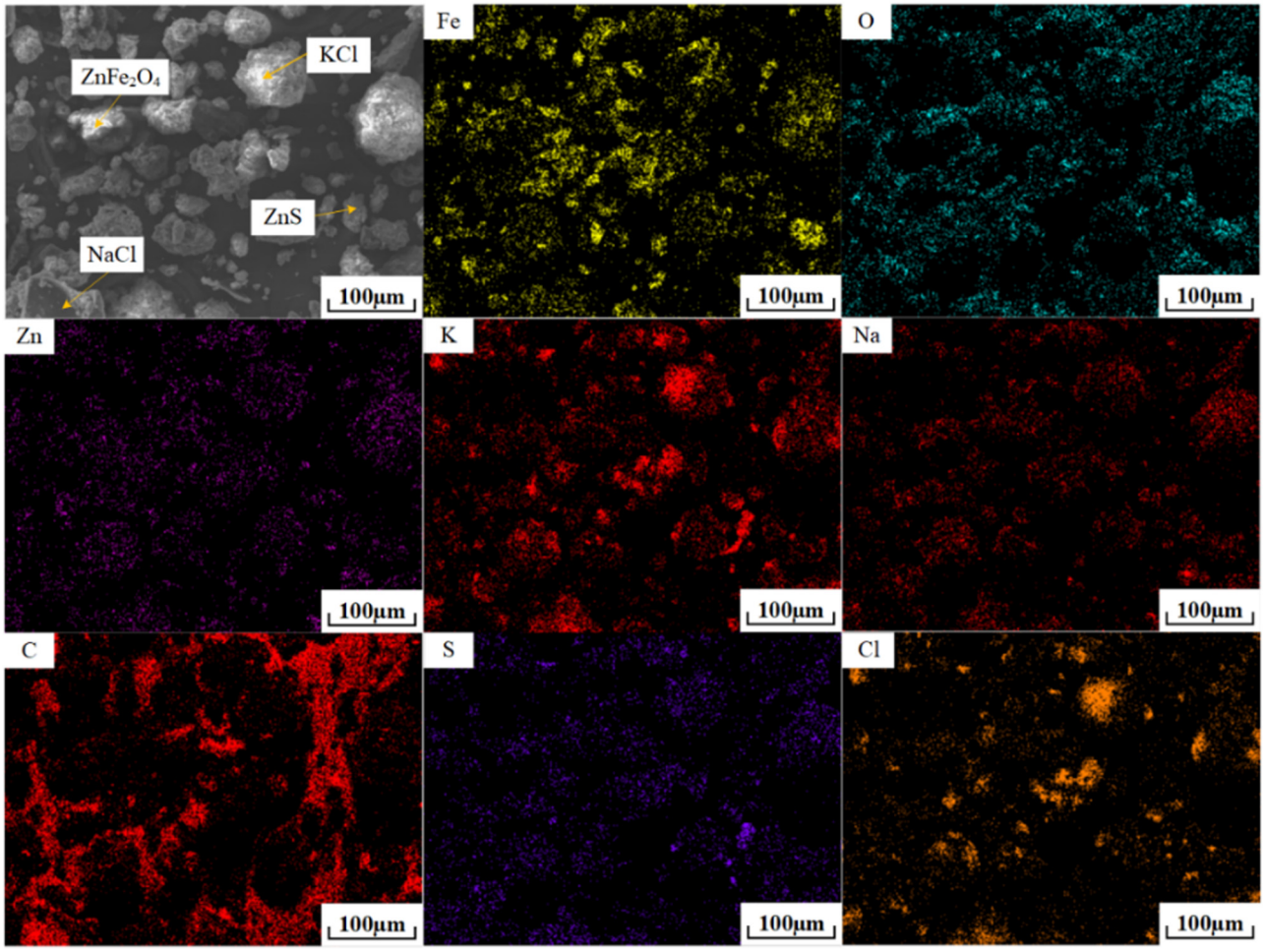

Figure 2: SEM-EDS images of BF dust.

Table 2: Raw material ratios of pre-reduction sintering experiments (wt%)

BF dust content (%)	ZC	GHL	NM	BF dust	Quicklime	Limestone	C
10	45.48	12.58	5.39	8.99	4.49	12.94	10.12
15	42.01	12.61	5.40	13.51	4.50	12.03	9.94
20	37.69	12.65	5.42	18.07	4.52	12.01	9.63
25	33.35	12.70	5.44	22.67	4.53	12.00	9.31
30	28.97	12.74	5.46	27.30	4.55	11.98	8.99

Note: The data in the table are normalized.

time. The reduction temperature (1,100°C, 1,150°C, 1,200°C, 1,250°C, and 1,300°C) and reduction time (0, 5, 10, 20, and 30 min) were, respectively, changed under the condition of 20% BF dust content. Once the reaction reaches the specified temperature and holding time, the porcelain boat is quickly removed, and the briquettes are covered with graphite powder to isolate the air and prevent secondary oxidation. The temperature rise curve of the pre-reduction sintering experiment is shown in Figure 3.

After the samples were cooled to room temperature, the content of metallic iron was determined by the ferric chloride-sodium acetate titration method (GB/T 6730.6-2016), and the content of Zn, K, and Na was determined by FAAS. The samples should be dissolved before the determination by FAAS as follows: accurately weigh 0.5000 g of the ground and dried sample into a 150 mL polytetrafluoroethylene beaker and wet it with a small amount of distilled water. Add 10 mL of hydrochloric acid (HCl) to heat

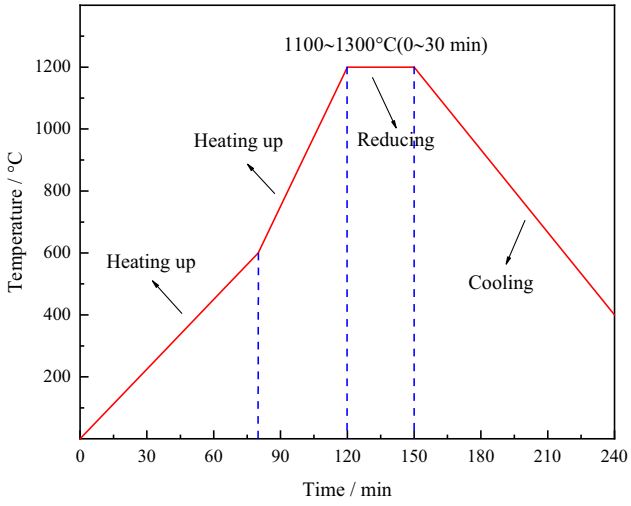

Figure 3: The temperature curve of pre-reduction sintering.

it for dissolution. After slightly cooling, add 5 mL of hydrofluoric acid, perchloric acid, and nitric acid, respectively. Cover the watch glass, heat it at a low temperature, and shake the beaker from time to time until the reaction stops. Remove the watch glass, raise the temperature, evaporate until white smoke comes out, take it down and cool it slightly, add 10 mL (1 + 1) HCl and 10 mL of distilled water to heat it to a slight boil and keep it for 2 min to dissolve the salt, transfer it to a 100 mL plastic volumetric flask, dilute it with water to the scale, and shake it evenly. When the ion concentration to be measured is high, it needs to be diluted before measurement.

FAAS are from Shimadzu Hong Kong Limited, and the equipment model is AA-6800. XRD analysis was conducted using a D8 Advance Diffractometer (Bruker, Billerica, MA, USA), with Cu Ka used as the radiation source (40 kV, 400 mA), the speed of scanning was 1°·min^{-1}, and at the range of 20–90° (2θ). An SU8010 field-emission scanning electron microscope (VEGA 3 XMU/XMH, Tescan, Czech Republic) was used for SEM imaging and EDX of pre-reduction sintered products, and the accelerating voltage was set to 15 kV.

The removal rate (ξ_i) of Zn, K, and Na in the pre-reduced sintered products can be calculated by the following expression:

$$\xi_i = \left(1 - \frac{M_i}{M_{i0}}\right) \times 100\% \quad (1)$$

where M_{i0} and M_i represent the total mass of each element in the initial briquettes and pre-reduction sintering products (%), respectively.

The metallization rate (η) of pre-reduction sintered products can be defined as follows:

$$\eta = \frac{M_{Fe}}{T_{Fe}} \times 100\% \quad (2)$$

where M_{Fe} and T_{Fe} refer to the mass fractions of metallic iron and total iron, respectively, in the pre-reduced sinter (%).

3 Results and discussion

3.1 Effect of BF dust content on pre-reduction sintering of briquettes

The effects of BF dust content on the Zn, K, and Na removal rates and metallization rate of the briquettes are shown in Figure 4. It can be seen that the Zn removal rate and metallization rate increase with the increase in dust content. Regardless of the dust content, the Zn removal rate always remained above 90%, and the metallization rate remained above 80%, which were both high levels. Both of them reached 97.57% and 87.14% at 30% dust ash content, respectively. On the contrary, the K and Na removal rates showed a trend of increasing and then decreasing with the increase in dust content, but the overall trend was increasing. The removal rate of both elements reached a high level at 25% of dust content, 83.57% and 94.78%, respectively.

The increase in BF dust content means an increase in harmful elements in raw materials. The increase in zinc content will lead to more zinc oxides in contact with the reducing agent, and more and more Zn will be reduced and volatilized, so the Zn removal rate will increase. The removal rate of K and Na increases with the increase in K

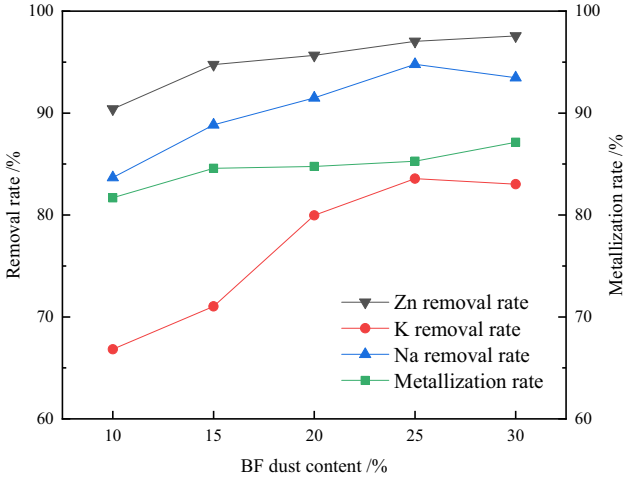

Figure 4: Effect of BF dust content on the removal rate and metallization rate of pre-reduction sintered products.

and Na content, which may be due to the fact that the main form of K and Na in BF dust is unstable chloride, which is easy to remove by heat at high temperatures. The reduction of iron oxides has little relation to the reduction of zinc oxides and the volatilization of KCl and NaCl, so the metallization rate is not much affected by the dust content.

3.2 Effect of temperature on pre-reduction sintering of briquettes

The effects of reduction temperature on the Zn, K, and Na removal rates and metallization rate of the briquettes with 20% BF dust content are shown in Figure 5. During the pre-reduction sintering process, the Zn removal rate increased slowly with the increase in temperature. and remained above 90% regardless of the temperature. When the temperature was increased from 1,100°C to 1,300°C, the Zn removal rate increased from 90.29% to 97.97%. In contrast, the K and Na removal rates were lower at 1,100°C, both less than 70%. As the temperature increased to 1,250°C, the K and Na removal rates increased significantly, with the K removal rate reaching over 85% and the Na removal rate reaching over 90%. When the temperature was increased to 1,300°C, the K and Na removal rates reached a high level of 93.76% and 94.97%, respectively. The metallization rate also increased from 75.98% to 89.47% during the process of increasing the reduction temperature from 1,100°C to 1,300°C, which could meet the requirements of subsequent BF production. It can be seen that the reduction temperature has a great influence on the metallization of agglomerates and Zn, K, and Na removal.

Figure 6 shows the XRD pattern of the pre-reduction sintered product with reduction temperature. As can be seen from Figure 6, as reduction temperature increases, the peaks of metallic iron become higher and higher, the content of metallic iron increases, and the peaks of $ZnFe_2O_4$ and KCl and NaCl become lower and even disappear. Figure 7 shows the SEM images and EDS maps of the pre-reduction sintered products at different reduction temperatures. As can be seen from Figure 7, with the increase in reduction temperature, the iron particles become larger and larger, and the pre-reduction sintered products become denser and denser. At the same time, the harmful elements Zn, K, and Na are becoming less and less prevalent and are gradually removed with the increase in temperature. The results of XRD and SEM are consistent with the above analysis. The metallization rate and the removal rate of harmful elements from pre-reduced sinter increase with the increase in reduction temperature.

Temperature has a great influence on the rate of gas diffusion, and there are pores in the briquettes themselves. Therefore, increasing temperature within a certain range has a positive influence on the reduction of briquettes. When the reduction time is certain, with the increase in the reduction temperature, the activity of materials participating in the reduction reaction and the molecular movement between the reaction gases are enhanced, and the iron-containing oxides and zinc-containing oxides in the briquettes will have a violent reduction reaction with solid carbon particles, and the metallization rate and zinc removal rate can be rapidly increased [18–20]. However, if the temperature continues to rise, the metal iron from the reduction of part of the magnetite in the surface

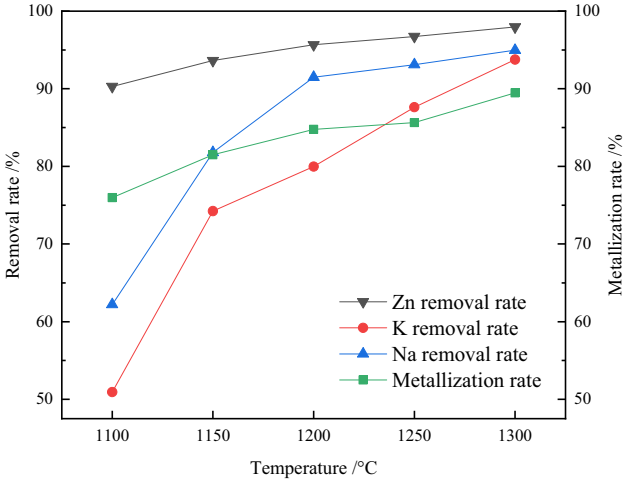

Figure 5: Effect of temperature on removal rate and metallization rate of pre-reduction sintered products.

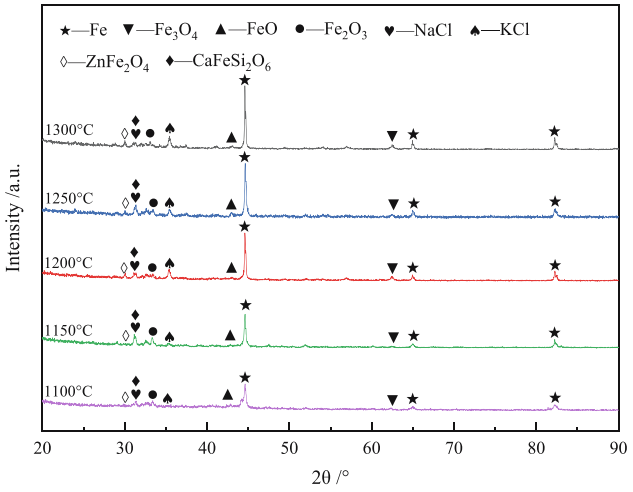

Figure 6: Effect of temperature on phase change of pre-reduction sintered products.

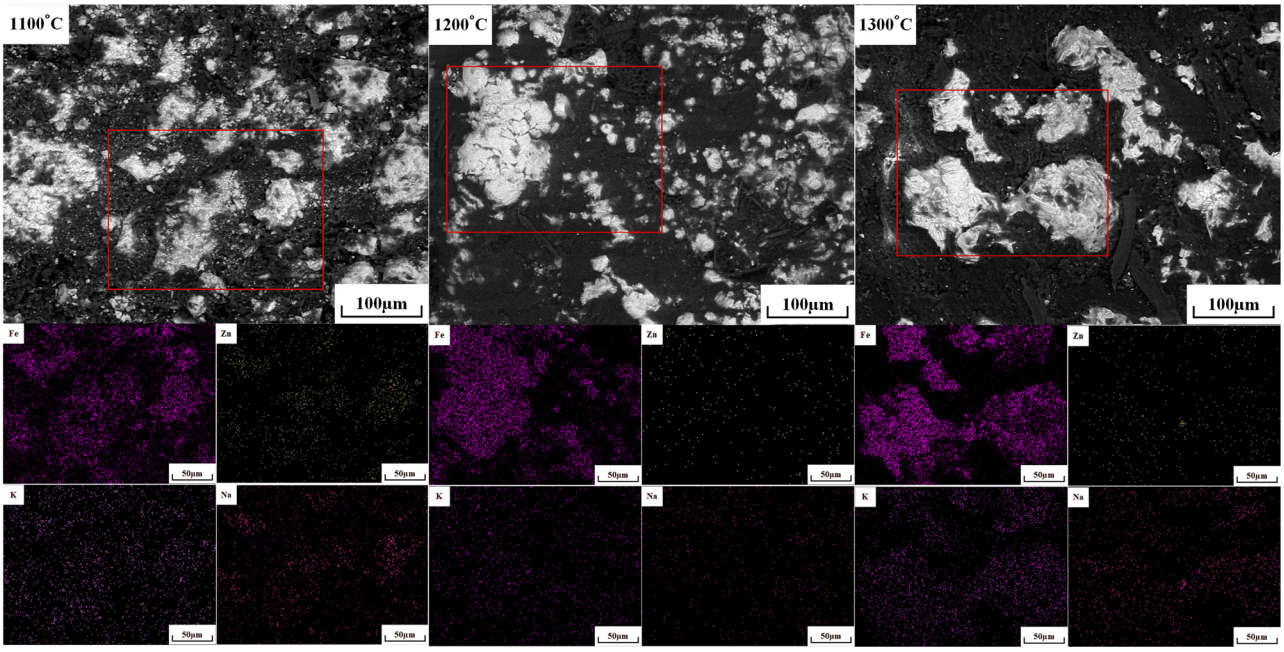

Figure 7: Effect of temperature on microstructure of pre-reduction sintered products.

layer of the mass may produce a relatively dense metal shell covering the periphery of the unreduced mineral powder, which hinders the diffusion of the reducing gas. In addition, the reduced FeO in mineral powder is easy to combine with SiO_2 to form low melting point liquid phase ferriolivine ($2FeO{\cdot}SiO_2$) [35], which is also easy to cause the blockage of pores and cracks inside the mass, and also hinder the diffusion of reducing gas, making it difficult to further improve the metallization rate and zinc removal rate. With the increase in temperature, the molecular movement of KCl and NaCl will also become faster, and more and more KCl and NaCl will be volatilized, so the removal rate of K and Na will increase with the increase in temperature.

3.3 Effect of time on pre-reduction sintering of briquettes

The effects of reduction time on the Zn, K, and Na removal rates and metallization rate of the briquettes with a dust content of 20% are shown in Figure 8. It can be seen that the reduction time has a great effect on pre-reduction sintering, and both metallization rate and removal rate increase with reduction time. The removal rates of three elements increased from 81.90%, 65.52%, and 78.89% at 0 min to 96.77%, 88.23%, and 95.57% at 30 min, respectively. The metallization rate remained above 80% and changed little with the reduction time. The metallization rate increased from 81.03% to 89.30% with the increase in reduction time from 0–30 min.

Figure 9 shows the XRD patterns of the pre-reduction sintered products with reduction time. As can be seen from Figure 9, the peaks of metallic iron become higher and higher as reduction time goes on, the content of metallic iron becomes higher and higher, and the peaks of $ZnFe_2O_4$, KCl, and NaCl become lower and even disappear. This is because hematite and magnetite are reduced to metallic iron, zinc ferrite is reduced to zinc vapor and then volatilized, and NaCl and KCl are also volatilized. Therefore, the

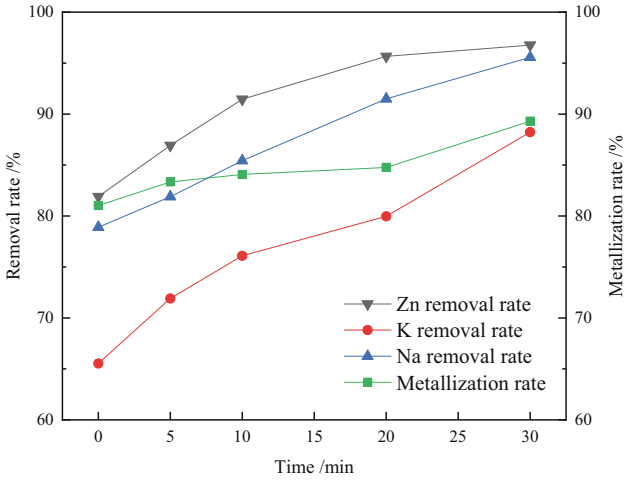

Figure 8: Effect of reduction time on removal rate and metallization rate of pre-reduction sintered products.

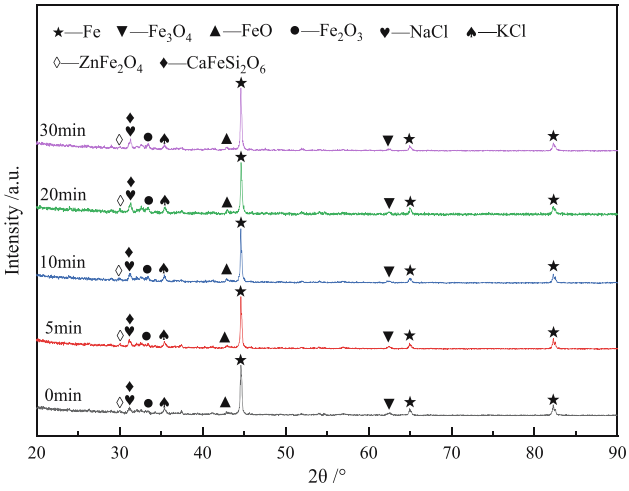

Figure 9: Effect of time on phase change of pre-reduction sintered products.

metallization rate and the removal rate of Zn, K, and Na are increased. Figure 10 shows the SEM images and the EDS maps of the pre-reduced sintered products at different reduction times. As can be seen from Figure 10, with the extension of reduction time, the iron oxides in the briquettes are continuously reduced, the metal iron grains increase and grow, and the fine iron grains aggregate to form larger iron grains, increasing the metallization rate of the briquettes. At the same time, Zn, K, and Na also decreased gradually with the extension of reduction time, and the removal rate of harmful elements gradually increased. XRD and SEM results can confirm the above analysis results.

Under the conditions of constant BF dust content, reduction temperature, and other factors, prolonging the reduction time in a reasonable range can make the reducing agent fully contact the mixed ore powder, and make the iron oxides, zinc oxides, and reducing agent fully react. The longer the reduction time is, the more full the reduction reaction will be; more iron and zinc will be reduced, and the Zn removal rate and metallization rate will increase. At the same time, prolonging the reduction time will make the KCl and NaCl fully volatilized, and the removal rate of K and Na will also increase. However, if the reduction time is further extended, it may have little impact on the Zn, K, and Na removal rate and metallization rate, and may even make them show a downward trend. This may be because with the extension of the reduction time, carbon is gradually consumed, and the reducing atmosphere in the furnace is weakened, so that the reduced iron and zinc are reoxidized.

3.4 Removal mechanism

The XRD pattern of BF dust shows that the main form of zinc is zinc ferrite ($ZnFe_2O_4$). The decomposition of zinc ferrite is as follows [36]:

$$ZnFe_2O_4 \rightarrow ZnO + Fe_2O_3 \quad (3)$$

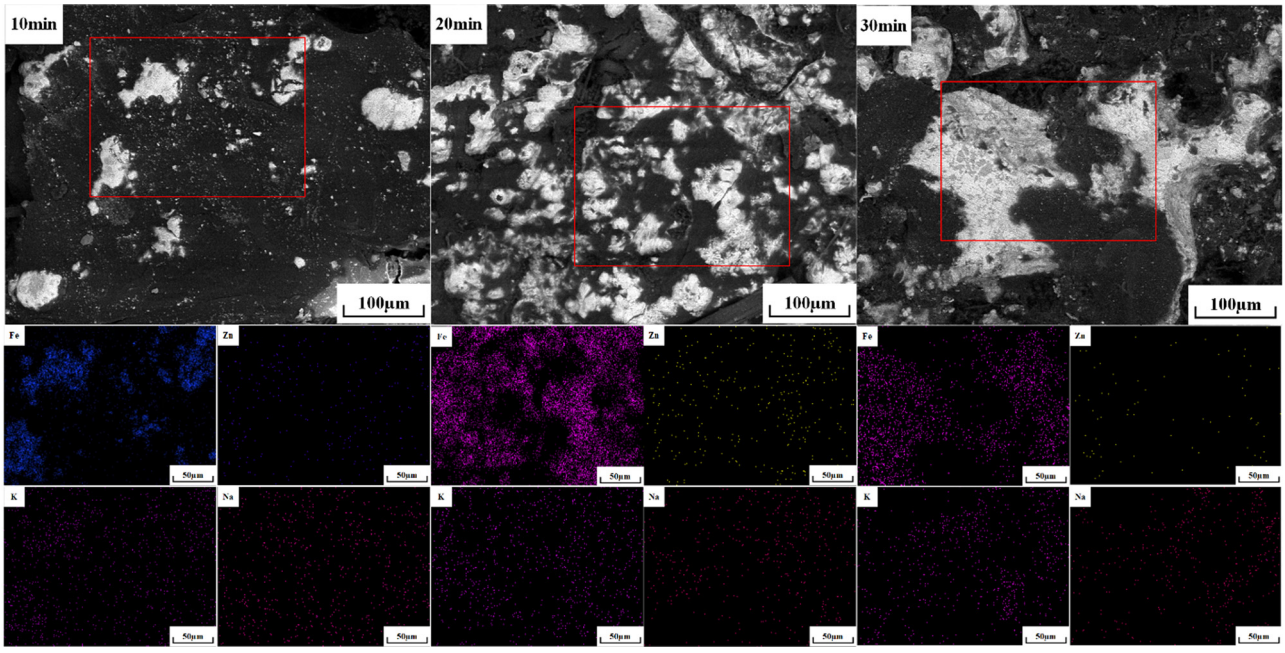

Figure 10: Effect of time on the microstructure of pre-reduction sintered products.

In the process of pre-reduction sintering, the reduction and volatilization of zinc mainly involve the following reactions:

$$C(s) + CO_2(g) = 2CO(g) \quad (4)$$

$$3ZnFe_2O_4(s) + C(s) = 3ZnO(s) + 2Fe_3O_4(s) + CO(g) \quad (5)$$

$$3ZnFe_2O_4(s) + CO(g) = 3ZnO(s) + 2Fe_3O_4(s) + CO_2(g) \quad (6)$$

$$ZnO(s) + C(s) = Zn(g) + CO(g) \quad (7)$$

$$ZnO(s) + CO(g) = Zn(g) + CO_2(g) \quad (8)$$

The decomposition of zinc ferrite is easier at high temperatures. The reduction mechanism of decomposed zinc ferrite is the same as that of zinc oxide (ZnO). In the process of pre-reduction sintering, there are two forms of reduction of metal oxides by solid carbon reducing agents. One is a direct reduction between solid and solid through solid carbon (C), and the other is an indirect reduction between gas and solid through carbon monoxide (CO). For the more stable metal oxides, direct reduction reactions dominate, while for the less stable metal oxides, indirect reduction reactions dominate. At the beginning of the pre-reduction reaction, a large amount of carbon monoxide has not been generated, so carbon is the main reducing agent. The reduction reaction between metal oxide and solid carbon is more favorable than the indirect reduction reaction, and the direct reduction reaction Eqs. 5 and 7 mainly occur. Zinc ferrite is first reduced to zinc oxide and magnetite, while producing carbon monoxide. With the pre-reduction reaction, carbon in the formed coal is gradually consumed, and carbon monoxide is also produced by the Boudouard reaction (Eq. 4). In a reducing atmosphere, the reduction of zinc ferrite is dominated by Eq. 6. At the same time, Eq. 8 occurs, more zinc oxide is reduced to zinc vapor, and then evaporation is achieved. In addition to zinc ferrite, there is a small amount of ZnS in BF dust. Some Zn may also be reduced by ZnS. The reduction reactions that may be involved are as follows:

$$ZnS(s) + C(s) = Zn(g) + CS(g),\ \Delta G^{\theta} = 606{,}312 - 293.3T \quad (9)$$

$$ZnS(s) + CO(g) = Zn(g) + COS(g),\ \Delta G^{\theta} = 297{,}802 - 125.8T \quad (10)$$

The Eq. 9 is an indirect reduction reaction. When the temperature is below 1,126.85°C, the COS in the gas phase is almost 0, indicating that the reaction is not easy to carry out. For the direct reduction, Eq. 10, the reaction temperature reaches 1,793.85°C in the standard state. Therefore, under normal solid-state reduction, the direct reduction of ZnS cannot be carried out. However, BF dust also contains a certain amount of CaO, and the entire study was conducted under high alkalinity conditions, so there is also the possibility that the following reactions may occur:

$$ZnS(s) + CaO(s) + CO(g) = Zn(g) + CaS(s) + CO_2(g),\ \Delta G^{\theta} = 205{,}191 - 124.5T \quad (11)$$

At higher temperatures, Eq. 11 occurs more readily than Eqs. 9 and 10, but under the same atmospheric conditions, Eq. 8 has a lower reaction temperature than Eq. 11. Eq. 8 proceeds preferentially over Eq. 11 [37]. This indicates that most of the Zn is reduced by $ZnFe_2O_4$ under the experimental conditions of this study, while a small amount of Zn may have been reduced by ZnS. Therefore, the removal of zinc can be simply described as $ZnFe_2O_4(s) \rightarrow ZnO(s) \rightarrow Zn(g)$ during the whole pre-reduction sintering process.

K and Na in the briquettes are in the form of chloride. KCl should be completely volatilized at 1,000°C, but KCl will react with SiO_2, Al_2O_3, and $CaCO_3$ at high temperatures [38]. Therefore, it is speculated that the minerals in iron concentrate and BF dust ash inhibit and delay the volatilization of KCl, but most of the volatilization of KCl can still be achieved with an increase in temperature and time. In a nitrogen atmosphere, NaCl also volatilizes after reaching the melting point. Thus, the removal of K and Na is actually attributable to the volatilization of KCl and NaCl at experimental temperatures.

4 Conclusion

1. The pre-reduction sintering process is an effective method for comprehensive utilization of BF dust, which can ensure a high metallization rate while removing harmful elements such as Zn, K, and Na from BF dust. It can avoid harmful elements in the BF and ensure smooth production.
2. With the increase in BF dust content, the Zn removal rate gradually increased, while the removal rates of K and Na showed a trend of first increasing and then decreasing. The removal rate of the three elements increased with the increase in reduction time and the increase in reduction temperature. When the BF dust content was 20%, the Zn, K, and Na removal rates in the reduction sintered products reached 95.66%, 79.97%, and 91.49%, respectively, after the briquettes were reduced at 1,200°C for 20 min. Most volatilization of Zn, K, and Na can be achieved by the pre-reduction sintering process.
3. With the increase in BF dust content, the prolongation of pre-reduction time, and the increase in pre-reduction temperature, the metallization rate of pre-reduction sintered products showed an increasing trend. When the

BF dust content is 20% and the briquettes are reduced at 1,200°C for 20 min, the metallization rate of the pre-reduction sintered products reaches 84.77%, which can meet the requirements of the subsequent BF production.

Funding information: The authors state no funding involved.

Author contributions: Guiqing Zhao: writing – original draft, writing – review and editing, methodology, and formal analysis; Ruoyan Li: writing – original draft, formal analysis, visualization, and project administration; Xiangdong Xing: writing – review and editing, methodology, and project administration; Jiantao Ju: conceptualization, data curation, and project administration; Xinyi Li: project administration; Jian Zu: project administration.

Conflict of interest: The authors state no conflict of interest.

Data availability statement: All data generated or analyzed during this study are included in this published article.

References

[1] Liu C, Zhang YZ, Wang F, Xu MX, Xing HW, Kang Y. Research status and prospect of multi-source metallurgical dust recycling. Chin Metall. 2022;32(10):38–44. doi: 10.13228/j.boyuan.issn1006-9356.20220365.

[2] She XF, Xue QG, Dong JJ, Wang JS, Zeng H, Li HF, et al. Study on basic properties of typical industrial dust from iron and steel plant and analysis of its utilization. Chin J Process Eng. 2009;9(S1):7–12. doi: 10.3321/j.issn:1009-606X.2009.z1.002.

[3] Liu P, Cao K. Discussion on the utility of dust and sludge containing zinc and iron from iron and steel plant. World Iron Steel. 2013;13(4):20–6. doi: 10.3969/j.issn.1672-9587.2013.04.005.

[4] Zhu DQ, Li SW, Pan J, Yang CC, Shi BJ. Migration and distributions of zinc, lead and arsenic within sinter bed during updraft pre-reductive sintering of iron-bearing wastes. Powder Technol. 2019;342:864–72. doi: 10.1016/j.powtec.2018.10.050.

[5] Shang HX, Li HM, Wei RF, Long HM, Li K, Liu WC. Present situation and prospect of iron and steel dust and sludge utilization technology. Iron Steel. 2019;54(3):9–17. doi: 10.13228/j.boyuan.issn0449-749x.20180431.

[6] An XW, Wang JS, She XF, Guo QG. Mathematical model of the direct reduction of dust composite pellets containing zinc and iron. Int J Min Metall Mater. 2013;20:627–35. doi: 10.1007/s12613-013-0776-6.

[7] Zhao YC, Robert S. Integrated hydrometallurgical process for production of zinc from electric arc furnace dust in alkaline medium. J Hazard Mater. 2000;80(1–3):223–40. doi: 10.1016/S0304-3894(00)00305-8.

[8] Petteri H, Joseph H, Hannu R, Mari L. Selection of leaching media for metal dissolution from electric arc furnace dust. J Clean Prod. 2017;164:265–76. doi: 10.1016/j.jclepro.2017.06.212.

[9] Peng HL. Study on the behavior of zinc ferrite in conventional hydrometallurgical zinc production process. Hunan Nonferrous Met. 2004;20(5):20–2. doi: 10.3969/j.issn.1003-5540.2004.05.007.

[10] Lin XL, Peng ZW, Yan JX, Li ZZ, Hwang JY, Zhang YB, et al. Pyrometallurgical recycling of electric arc furnace dust. J Clean Prod. 2017;149:1079–100. doi: 10.1016/j.jclepro.2017.02.128.

[11] Lu J. Technical research on treatment of zinc and iron containing dust and sludge. Sinter. Pellet. 2011;36(6):50–2. doi: 10.13403/j.sjqt.2011.06.014.

[12] Palencia I, Romero R, Iglesias N, Carranza F. Recycling EAF dust leaching residue to the furnace: A simulation study. JOM-J Min Met Mat S. 1999;51(8):28–32. doi: 10.1007/s11837-999-0238-9.

[13] Kometani A, Kawaguchi Y, Ohnishi M, Ono Y, Hashimoto T, Nakamura F. Dry removal method of zinc from blast furnace dry dust. Tetsu Hagane. 1985;71(15):1759–64. doi: 10.2355/tetsutohagane1955.71.15_1759.

[14] Das B, Prakash S, Reddy PSR, Misra VN. An overview of utilization of slag and sludge from steel industries. Resour Conserv Recycl. 2007;50(1):40–57. doi: 10.1016/j.resconrec.2006.05.008.

[15] Cheng XL, Zhao K, Qi YH, Shi XF, Zhen CL. Direct reduction experiment on iron-bearing waste slag. J Iron Steel Res Int. 2013;20(3):24–29,35. doi: 10.1016/S1006-706X(13)60064-3.

[16] Lanzerstorfer C, Bamberger-Strassmayr B, Pilz K. Recycling of blast furnace dust in the iron ore sintering process: Investigation of coke breeze substitution and the influence on off-gas emissions. ISIJ Int. 2015;55(4):758–64. doi: 10.2355/isijinternational.55.758.

[17] Zhang LF. Study on treatment of Zn-containing dust of iron and steel plants by Rotary Hearth Furnace process in China. Sinter Pellet. 2012;37(3):57–60. doi: 10.13403/j.sjqt.2012.03.017.

[18] Peng C, Zhang FL, Li HF, Guo ZC. Removal behavior of Zn, Pb, K and Na from cold bonded briquettes of metallurgical dust in simulated RHF. ISIJ Int. 2009;49(12):1874–81. doi: 10.2355/isijinternational.49.1874.

[19] Xia LG, Mao R, Zhang JL, Xu XN, Wei MF, Yang FH. Reduction process and zinc removal from composite briquettes composed of dust and sludge from a steel enterprise. Int J Min Met Mater. 2015;22(2):122–31. doi: 10.1007/s12613-015-1052-8.

[20] She XF, Wang JS, Wang G, Xue QG, Zhang XX. Removal mechanism of Zn, Pb and Alkalis from metallurgical dusts in direct reduction process. J Iron Steel Res Int. 2014;21(5):488–95. doi: 10.1016/S1006-706X(14)60076-5.

[21] Zhu DQ, Wang DZ, Pan J, Tian HY, Xue YX. A study on the zinc removal kinetics and mechanism of zinc-bearing dust pellets in direct reduction. Powder Technol. 2021;380:273–81. doi: 10.1016/j.powtec.2020.11.077.

[22] Ma HY, Pei YD, Pan W, Chen SG. Characteristic and recycling progress of dust in sintering machine head. Chin Metall. 2018;28(6):5–8,12. doi: 10.13228/j.boyuan.issn1006-9356.20180052.

[23] Kang LC, Zhang L, Zhang DH, Huang JY, Xue GF. Treatment and utility of the electrostatic precipitator dust of the sintering machine. Ind Saf Environ Prot. 2015;41(3):41–3. doi: 10.3969/j.issn.1001-425X.2015.03.013.

[24] Bi XG, Wang YY, Xie DG, Liu W, Zhou JD. Experimental study on production of carbon-blended pellets with using sinter ESP dusts. Sinter Pellet. 2017;42(01):38–44. doi: 10.13403/j.sjqt.2017.01.009.

[25] Yang JF, Wang X, Zhang YC, Li XF. Equilibrium analysis and elimination of harmful element in blast furnace. Chin Metall.

2007;17(11):35–40. doi: 10.13228/j.boyuan.issn1006-9356.2007.11.010.
[26] Wang DY, Wang WZ, Chen WQ, Zhou RZ, Lin ZC. Present state and development trend of disposal technique of in-plant Zn-Pb-Bearing dust. Iron Steel. 1998;33(1):67–70. doi: 10.3321/j.issn:0449-749X.1998.01.017.
[27] Yu H, Huang XC, Li K, Li Q. Present situation and prospect of comprehensive utilization of precipitator dust in iron and steel enterprises. Conserv Util Min Resour. 2021;41(04):164–71. doi: 10.13779/j.cnki.issn1001-0076.2021.07.009.
[28] Hu JG, Wang ZY, Chen Y, Zhou WT, Guo YL. New ironmaking technology of reducing CO_2 of Japanese steel industry. World Iron Steel. 2011;11(3):1–4. doi: 10.19537/j.cnki.2096-2789.2011.03.015.
[29] Ariyama T, Sato M. Optimization of ironmaking process for reducing CO_2 emissions in the integrated steel works. ISIJ Int. 2006;46(12):1736–44. doi: 10.2355/isijinternational.46.1736.
[30] Kazuya K, Yasushi T, Yasuhiko F, Takashi O. Blast furnace ironmaking process using pre-reduced iron ore. Nippon Steel Tech Rep. 2006;94:133–8.
[31] Satoshi M, Hideaki S, Kanji T. Development of the process for producing pre-reduced agglomerates. JFE Tech Rep. 2009;13:7–13.
[32] Yabe H, Takamoto Y. Reduction of CO_2 emissions by use of pre-reduced iron ore as sinter raw material. ISIJ Int. 2013;53(9):1625–32. doi: 10.2355/isijinternational.53.1625.
[33] Sato H, Machida S, Nushiro K, Ichikawa K, Sato M, Ariyama T, et al. Development of production process for pre-reduced agglomerate and evaluation of its quality. Tetsu Hagane. 2006;92(12):815–24. doi: 10.2355/tetsutohagane1955.92.12_815.
[34] Hu B, Gan M, Wang ZC. Experimental study on comprehensive utilization of dust in steel plants with pre-reduction sintering process. Sinter Pellet. 2018;43(6):38–42. doi: 10.13403/j.sjqt.2018.06.084.
[35] Zhang YY, Cui KK, Wang J, Wang XF, Qie JM, Xu QY, et al. Effects of direct reduction process on the microstructure and reduction characteristics of carbon-bearing nickel laterite ore pellets. Powder Technol. 2020;376:496–506. doi: 10.1016/j.powtec.2020.08.059.
[36] Guo T, Hu XJ, Matsuura H, Tsukihashi F, Zhou GZ. Kinetics of Zn removal from ZnO-Fe_2O_3-$CaCl_2$ system. ISIJ Int. 2010;50(8):1084–8. doi: 10.2355/isijinternational.50.1084.
[37] Guo PM, Zhao P. Efficient utilization of metallurgical resources. Beijing: Metallurgical Industry Press; 2012. pp. 245–246.
[38] Kai XP, Yang TH, Sun Y, He YG, Li RD, Wei LH. Study on migration mechanism of alkali metals during co-firing of rice straw and coal. Proc CSEE. 2012;32(8):133–8. doi: 10.13334/j.0258-8013.pcsee.2012.08.016.